Chin. J. Astron. Astrophys. Vol. 3 (2003), No. 6, 576–586
(*http://www.chjaa.org* or *http://chjaa.bao.ac.cn*)

Chinese Journal of
Astronomy and
Astrophysics

A Tilt-correction Adaptive Optical System for the Solar Telescope of Nanjing University *

Chang-Hui Rao[1], Wen-Han Jiang[1], Cheng Fang[2], Ning Ling[1], Wei-Chao Zhou[1], Ming-De Ding[2], Xue-Jun Zhang[1], Dong-Hong Chen[1], Mei Li[1], Xiu-Fa Gao[2] and Tian Mi[2]

[1] Adaptive Optics Lab., Institute of Optics and Electronics, Chinese Academy of Sciences, P. O. Box 350, Chengdu 610209; chrao@sc.homeway.com.cn
[2] Astronomy Department, Nanjing University, Nanjing 210093

Received 2003 March 24; accepted 2003 May 19

Abstract A tilt-correction adaptive optical system installed on the 430 mm Solar Telescope of Nanjing University has been put in operation. It consists of a tip-tilt mirror, a correlation tracker and an imaging CCD camera. An absolute difference algorithm is used for detecting image motion in the correlation tracker. The sampling frequency of the system is 419 Hz. We give a description of the system's configuration, an analysis of its performance and a report of our observational results. A residual jitter of 0.14 arcsec has been achieved. The error rejection bandwidth of the system can be adjusted in the range 5–28 Hz according to the beacon size and the strength of atmospheric turbulence.

Key words: telescopes — atmospheric effects — instrumentation — adaptive optics — Sun: atmospheric motions

1 INTRODUCTION

It is well known that random image motion induced by atmospheric turbulence and mechanical vibrations of the telescope severely degrade the angular resolution of ground-based solar telescopes when the exposure time of the detector is longer than, or comparable to the time scale of the image motion. This motion can be detected with the use of solar granulation or sunspot as beacon and can be compensated in the isoplanatic area of the solar image by means of correlation tracking. Until now, a few correlation trackers (Ballesteros et al. 1996; Rao et al. 2001; Molodij et al. 1996; and von der Luehe et al. 1989) have been successfully developed for solar telescopes.

For low contrast and extended objects such as solar granulation, solar pores and sunspots, a correlation tracking algorithm has been verified (Rao et al. 2001). The absolute difference algorithm can be used for the measurement of solar image motion. We built a tilt-correction

* Supported by the National Natural Science Foundation of China.

adaptive optical system for the 430 mm Solar Telescope of Nanjing University. Table 1 lists the major specifications of correlation trackers for solar telescopes developed so far.

In this paper, the configuration of our system is described in Section 2. In Section 3, the observation results are reported. The performance of the system is analyzed in Section 4. Section 5 summarizes the major results.

Table 1 Major Specifications of Correlation Trackers for Solar Telescopes

Country	USA	France-Italy	Spain	China
Year	1989	1995	1995	2001
Diameter [mm]	760	900	980	430
Beacon	granulation	granulation	granulation	sunspot
Algorithm	cross correlation coefficient	granulation tracker	absolute difference	absolute difference
Sampling frequency [Hz]	417	582	1350	419
Field of view	$10'' \times 10''$	$2'' \times 2'' \sim 12'' \times 12''$	$14'' \times 14''$	$5'' \times 5'' \sim 20'' \times 20''$
Bandwidth [Hz]	25 (open-loop)	60 (close -3dB)	100 (open-loop)	30 (open-loop) 84 (close -3dB) 28 (error rejection)
Image quality	motion $0.023''$ rms	$0.2''$ resolution	motion $0.05''$ rms	motion $0.14''$ rms

2 DESCRIPTION OF THE TILT-CORRECTION ADAPTIVE OPTICAL SYSTEM

Figure 1 shows the optical setup of the Solar Telescope of Nanjing University. The main optical path is made up of the flat reflective mirror M1 and M2 (which is used for solar tracking), the spherical primary mirror M3, and the flat mirror M6. The effective aperture of the telescope is 430 mm and the focal length is 21.7 m. The size of the solar image in the primary focus F1 is about 20 cm. When the tilt-correction adaptive optical system is in operation, the flat mirror M6 is displaced by the tip-tilt mirror.

The tilt-correction adaptive optical system is shown in Fig. 2. It consists of a tip-tilt mirror, a correlation tracker and an imaging CCD camera.

2.1 Tip-tilt Mirror

Figure 3 shows the interferograms of the tip-tilt mirror before and after coating. The measurement wavelength is 632.8 nanometers. The frequency response curves of the tip-tilt mirror in the X direction and Y direction are plotted respectively in Fig. 4. The solid and dotted lines are the amplitude curve and phase curve respectively. It can be seen from Fig. 4 that the resonance frequencies of the tip-tilt mirrors in the X direction and Y direction are both about 480 Hz.

The tip-tilt mirror was developed in the Adaptive Optics Laboratory, Institute of Optics and Electronics, Chinese Academy of Sciences. Its specifications are as follows:

Type of actuators: PZT stack

Clear aperture: ϕ110 mm
Maximum tilt angle: $\pm$120 arcsec
Maximum voltage: $\pm$700 V
Surface: 0.015λ rms (λ=0.6328 μm)
Resonance frequency: $\sim$480 Hz

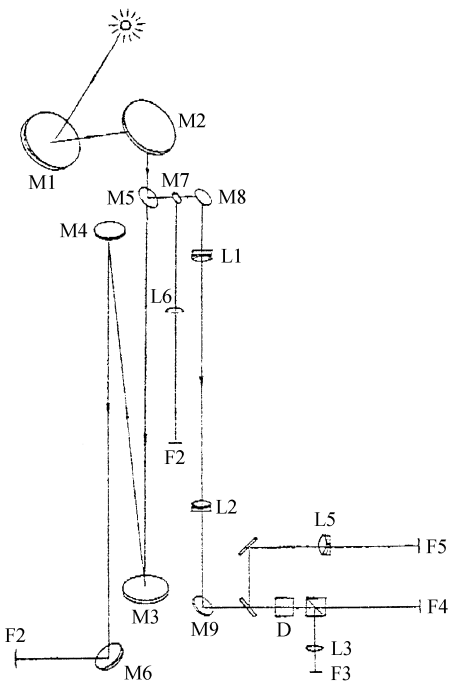

Fig. 1 Optical setup for Solar Telescope of Nanjing University.

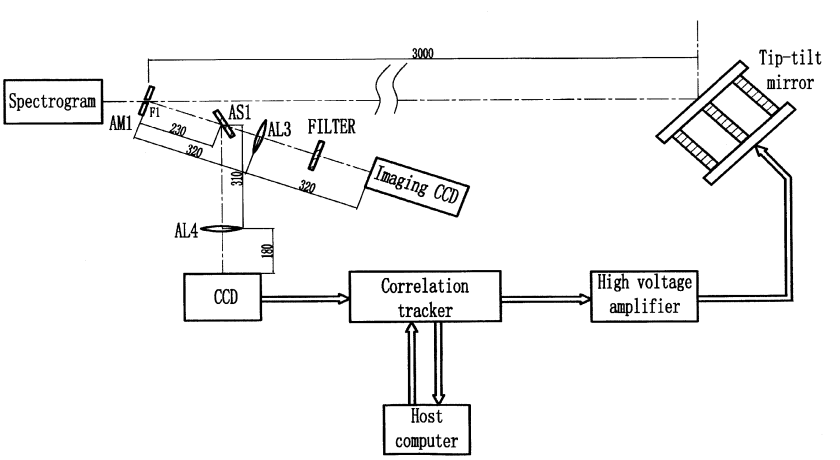

Fig. 2 Schematic diagram of the tilt-correction adaptive optical system.

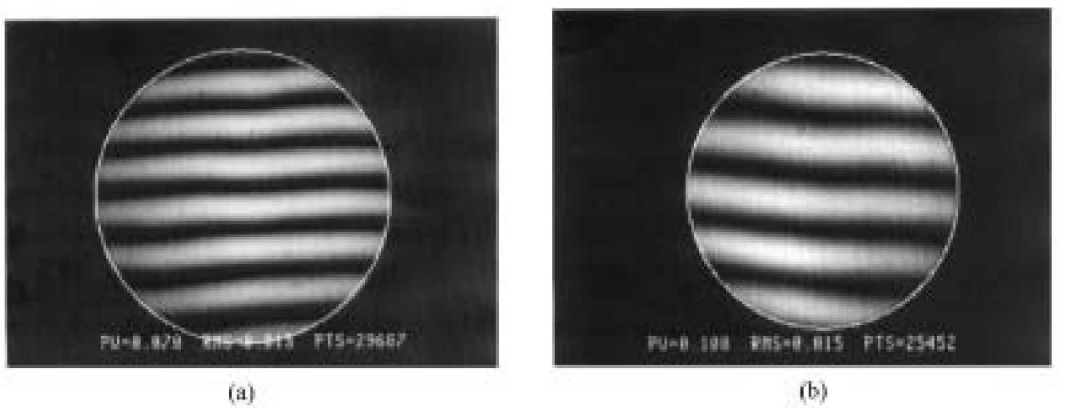

(a) (b)

Fig. 3 Interferograms of the tip-tilt mirror. (a) before coating; (b) after coating.

2.2 Correlation Tracker

The basic principle of correlation tracking is as follows. Using correlation techniques, successive images are compared with a previously stored reference image to determine their relative position displacement. These shifts constitute tilt error signals which are then applied to the tip-tilt mirror.

For the correlation tracker of this system, absolute difference algorithm is used for detecting the image motion induced by atmospheric turbulence and mechanical vibrations of the telescope. The algorithm proceeds as follows. First, it calculates the sum of the absolute differences between the reference image and the live image at different positions, then it searches the minimum in the entire field of view of the detector, which constitutes the tilt error signal. With N*N reference image I_R and the M*M live image $I_L(M < N)$, the absolute difference algorithm has the form

$$D_{LR}(u,v) = \sum_{i=0}^{M-1}\sum_{j=0}^{M-1} |I_R(i+u, j+v) - I_L(i,j)|, \tag{1}$$

where u and v are the position displacements between the reference and the live image in the horizontal and perpendicular directions, respectively.

Using a parabolic interpolation, the image motion signals with subpixel precision at the x and y directions can be obtained as (Rao et al. 2001):

$$TX = u_{\min} + \frac{1}{2}\frac{D_{LR}(u_{\min}+1, v_{\min}) - D_{LR}(u_{\min}-1, v_{\min})}{D_{LR}(u_{\min}-1, v_{\min}) + D_{LR}(u_{\min}+1, v_{\min}) - 2D_{LR}(u_{\min}, v_{\min})}, \tag{2}$$

and

$$TY = v_{\min} + \frac{1}{2}\frac{D_{LR}(u_{\min}, v_{\min}+1) - D_{LR}(u_{\min}, v_{\min}-1)}{D_{LR}(u_{\min}, v_{\min}-1) + D_{LR}(u_{\min}, v_{\min}+1) - 2D_{LR}(u_{\min}, v_{\min})}. \tag{3}$$

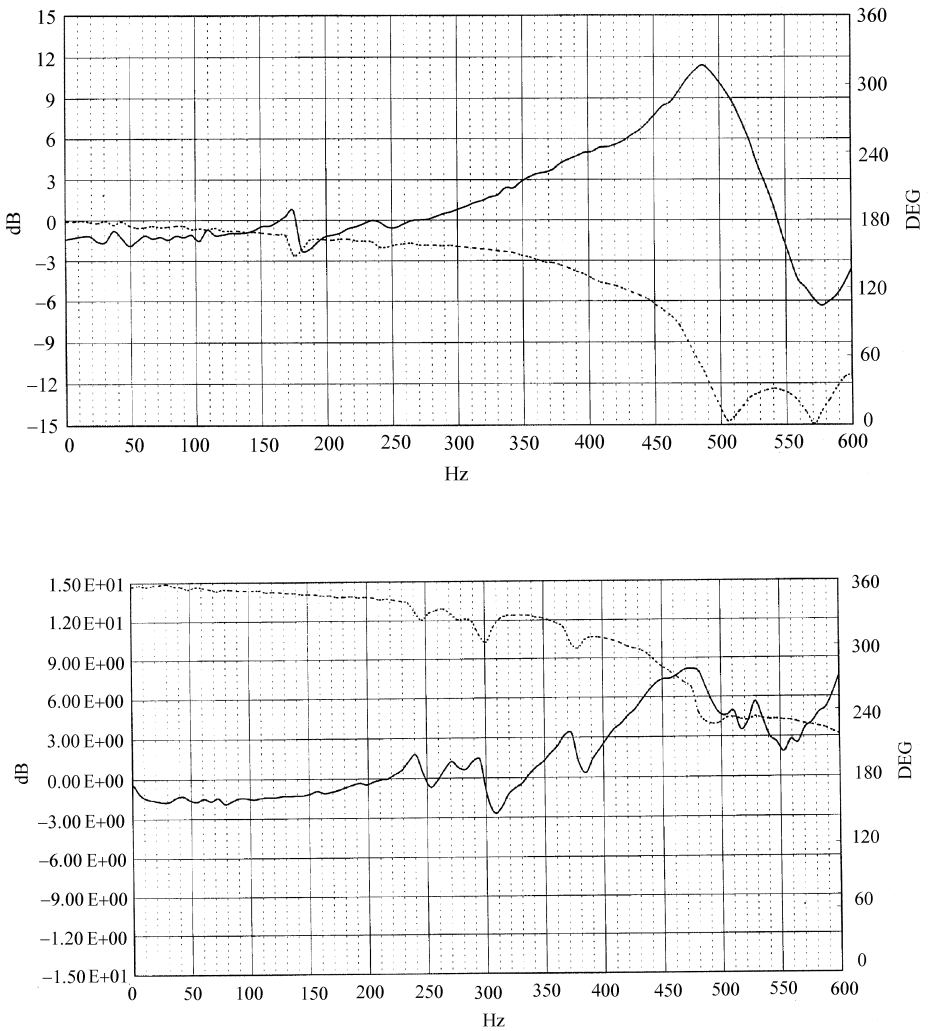

Fig. 4 Frequency response curves of the tip-tilt mirror. The solid and dotted lines are the amplitude and phase curves, respectively. (a) X direction; (b) Y direction.

In Eqs. (2) and (3), $u_{\min}$ and $v_{\min}$ represent the position displacements in the horizontal and perpendicular direction, respectively, when the sum of the absolute difference in the entire field of view is minimum.

In the tilt-correction adaptive optical system, the correlation tracker shown in Fig. 5 is made up of four parts: CCD image acquisition, correlation tracking algorithm, control algorithm and D/A converter. Its main functions are to compute and compare the sum of the absolute difference between the reference image and the live image at different positions, to finish the parabolic interpolation, and to perform the control algorithm. The computation of the sum of absolute differences between the reference image and the live image at different positions is accomplished by hardware with use of Field Programmable Gate Array (FPGA) Virtex-600E. The comparison of the sum of the absolute differences, the parabolic interpolation and

the control algorithm are executed by software with use of Digital Signal Processor (DSP) TMS320C30.

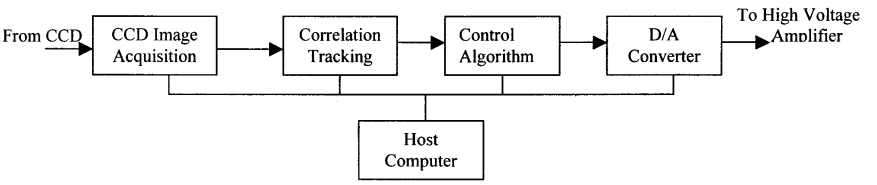

Fig. 5 Schematic diagram of the correlation tracker.

3 EXPERIMENTAL RESULTS

The tilt-correction adaptive optical system has been closed-looped in our laboratory in October 2001. In December 2001 the system was installed at the Solar Tower of Nanjing University and was successfully closed-looped for sunspot. Due to severe air pollution, solar granulation cannot be resolved at this site. In the experiment only solar pore and sunspot with high contrast can be used to realize correlation tracking. In the following we present some experimental results.

3.1 Control Characteristics of the System

The control transfer function of the tilt-correction adaptive optical system was measured. Figure 6 presents the measured open loop control transfer function curves of the system without control algorithm. The total delay time of the system is 2.8T (T is the sampling period).

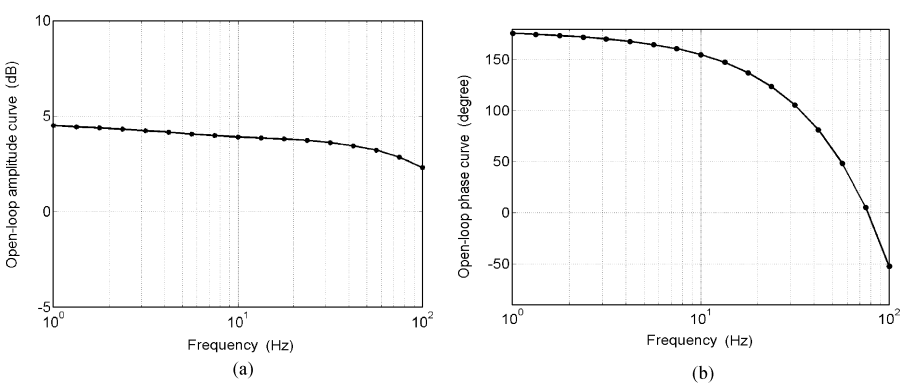

Fig. 6 Open loop control transfer function curves of the system without control algorithm. The total delay time of the system is 2.8T (T is the sampling period). (a) Open loop amplitude curve; (b) Open loop phase curve.

Figure 7 shows a set of control transfer function curves. The open loop bandwidth, the closed-loop –3dB bandwidth and the error rejection bandwidth are 30.4 Hz, 84 Hz and 27.5 Hz, respectively. The error rejection bandwidth of the system can be adjusted in the range from 5 Hz to 28 Hz according to the beacon size and the strength of the atmospheric turbulence.

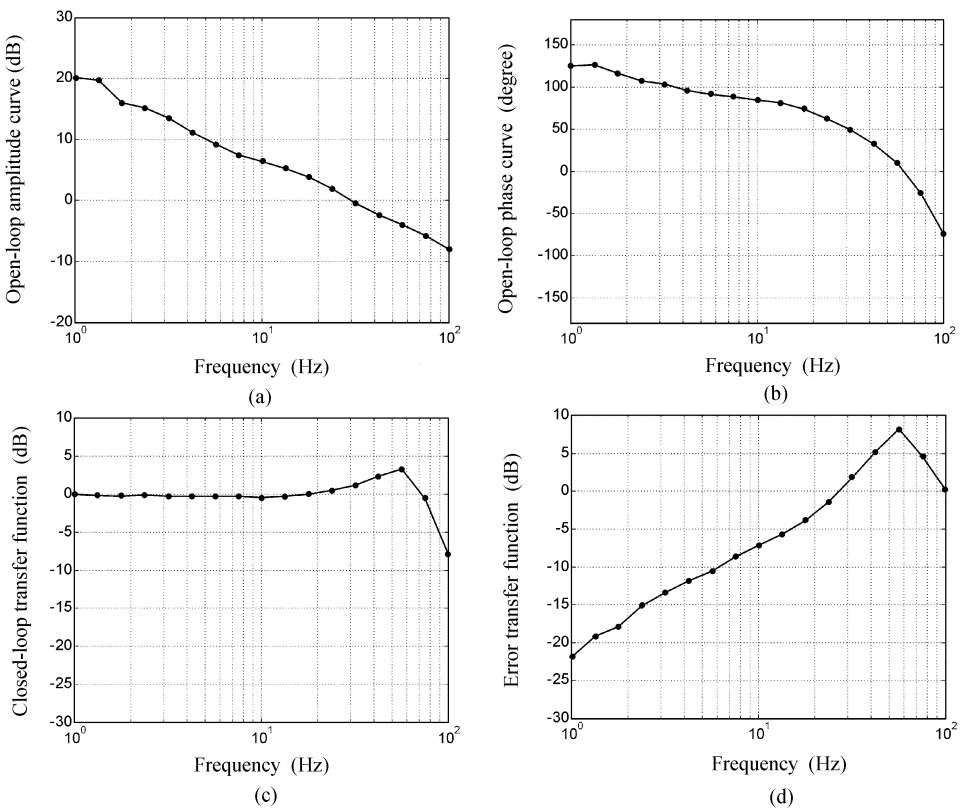

Fig. 7 Control transfer function curves of the tilt-correction adaptive optical system. (a) Open loop amplitude curve; (b) Open loop phase curve; (c) Closed-loop transfer function; (d) Error transfer function.

3.2 The Measured Image Motion

Figure 8 presents the time series of the measured open loop and closed-loop image motion. The rms value of the open loop image motion is 0.90 arcsec and 1.06 arcsec in X and Y directions, respectively. As the tilt-correction adaptive optical system is closed-loop, the residual image motion reduces to 0.19 arcsec and 0.14 arcsec in X and Y directions, respectively. The results show the very evident and effective improvement of the correlation tracking for image motion induced by atmospheric turbulence and mechanical vibrations of the telescope.

Figure 9 shows the power spectrum of the measured open loop and closed-loop image motion corresponding to Fig. 8. It can be seen that the low frequency part (below 16 Hz) of the image motion induced by atmospheric turbulence and mechanical vibrations of the telescope is compensated effectively. In this case, the error rejection bandwidth of the system is 16 Hz.

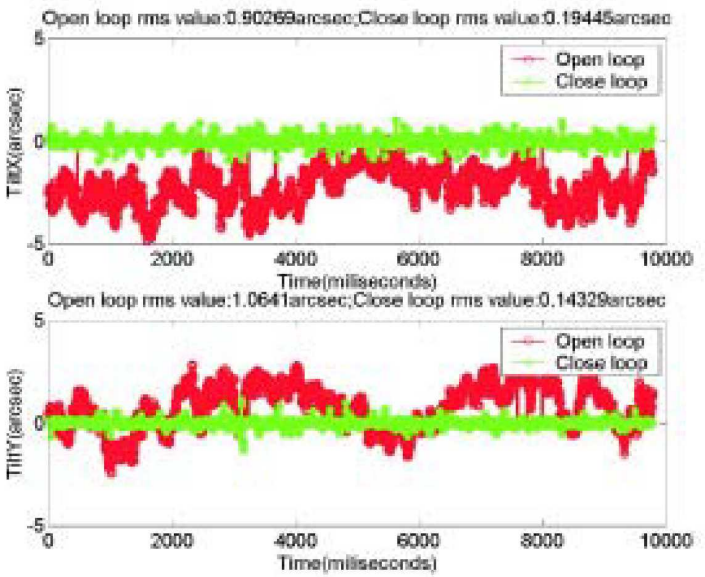

Fig. 8 Time series of measured open loop and closed-loop image motions.

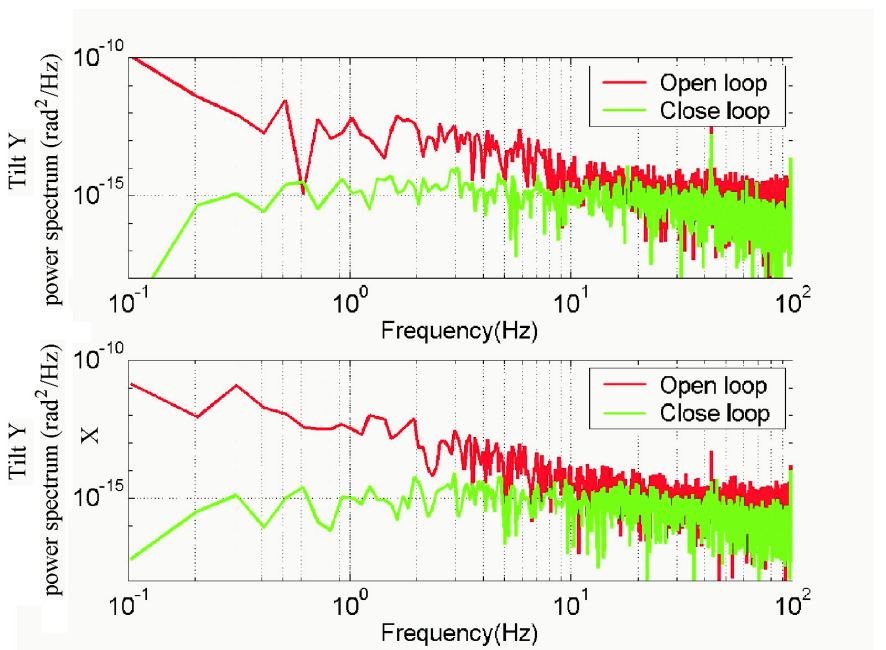

Fig. 9 Power spectrum of the measured open loop and closed-loop image motions corresponding to Fig. 8.

3.3 Long Exposure Solar Image

Figures 10 and 11 show two sets of open loop and closed-loop long exposure solar image. It can be seen that the closed-loop long exposure solar image has a certain improvement in contrast with the open loop solar image. In the experiment, the sunspot is used as the beacon for tilt correction. Due to the severe air pollution at this site, solar granulation cannot be resolved. Furthermore, the tracking precision of the correlation tracker is affected by the extension of the beacon. The smaller the extension of the beacon, the higher the tracking precision is, and the more effective the compensation is. So the improvement of the correlation tracking for image motion induced by atmospheric turbulence and mechanical vibrations of the telescope can become more evident if solar granulation can be resolved.

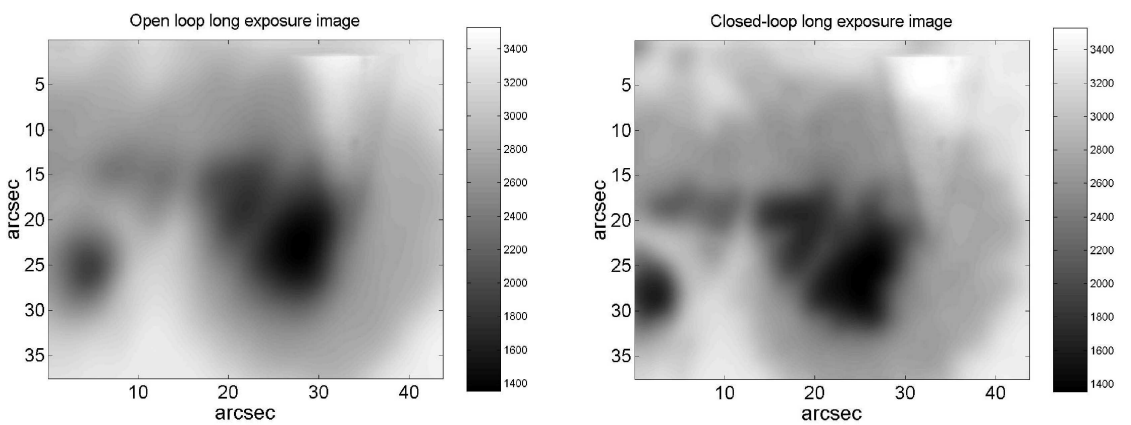

Fig. 10 Open-loop and closed-loop long exposure solar images.

4 PERFORMANCE ANALYSIS

In an adaptive optical system, the imaging performance depends on the tilt residual error and the higher-order error. For a tilt-correction adaptive optical system, however, the higher-order wavefront error induced by atmospheric turbulence can be expressed as

$$\sigma_{\text{fig}}^2 = 0.134 \left(\frac{D}{r_0}\right)^{5/3}, \tag{4}$$

where D is the diameter of the system, r_0 is the turbulence coherence length.

Accordingly, the resolutions of the tilt-correction adaptive optical system for short exposure imaging and long exposure imaging are, respectively,

$$RES_{\text{SE}} = \left(1.22\frac{\lambda}{D}\right) \Bigg/ \sqrt{\exp(-\sigma_{\text{fig}}^2) + \frac{1-\exp(-\sigma_{\text{fig}}^2)}{1+\left(D/r_0\right)^2}}, \tag{5}$$

and

$$RES_{LE} = \left(1.22\frac{\lambda}{D}\right) \Bigg/ \sqrt{\frac{\exp(-\sigma_{\rm fig}^2)}{1+5\left(D/\lambda\right)^2\sigma_{\rm tilt}^2} + \frac{1-\exp(-\sigma_{\rm fig}^2)}{1+\left(D/r_0\right)^2}}\,. \tag{6}$$

In Eqs. (5) and (6), $\sigma_{\rm tilt}^2$ and $\sigma_{\rm fig}^2$ are the tilt residual error and the higher-order wavefront error, respectively.

Figure 12 shows the imaging resolution of the system as function of the atmospheric coherence length for different tilt residual error. Obviously, the smaller the atmospheric coherence length, the larger the tilt residual error and the lower the imaging resolution is. We list the computed values of the imaging resolution of the system in Table 2.

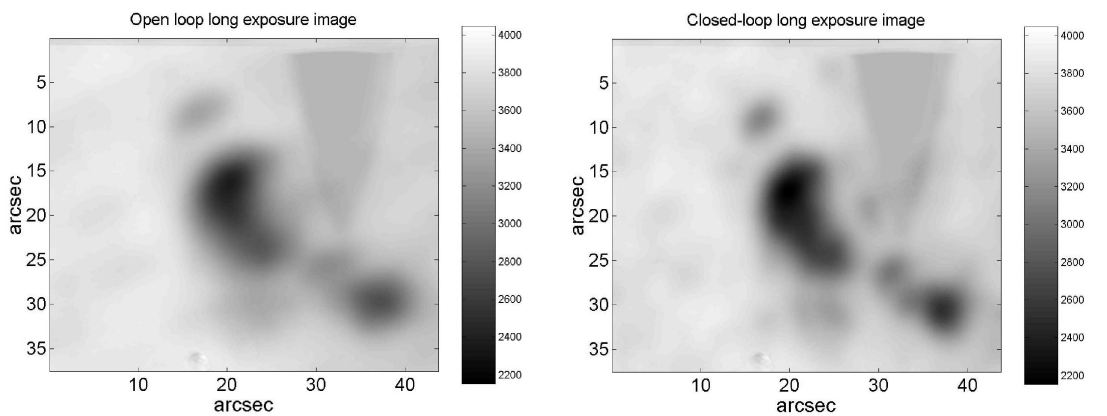

Fig. 11 Open loop and closed-loop long exposure solar images.

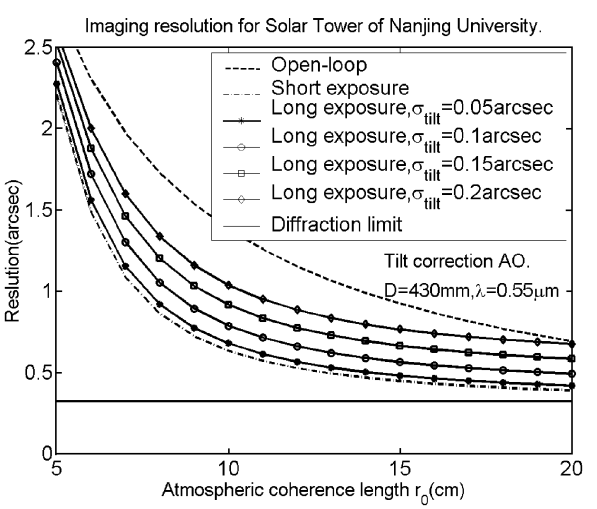

Fig. 12 Imaging resolution of the system vs. atmospheric coherence length for different tilt residual errors.

Table 2 Imaging Resolution of the System (unit: arcsec)

r_0 (cm)	Diffraction limit	Short exposure	Long exposure for different tilt rms error				Open loop
			$0.05''$	$0.1''$	$0.15''$	$0.2''$	
5	0.32	2.21	2.28	2.41	2.52	2.70	2.76
8	0.32	0.86	0.92	1.05	1.20	1.33	1.73
10	0.32	0.63	0.68	0.79	0.92	1.04	1.38
15	0.32	0.45	0.48	0.56	0.66	0.76	0.92

5 SUMMARY

We have built and installed a tilt-correction adaptive optical system at the 430 mm Solar Telescope of Nanjing University. It consists of a tip-tilt mirror, a correlation tracker and an imaging CCD camera. The configuration of the system has been described. An absolute difference algorithm is used for detecting image motion in the correlation tracker. As the tilt-correction adaptive optical system is closed-loop, the improvement of the correlation tracking for image motion induced by atmospheric turbulence and mechanical vibrations of the telescope is very evident and effective. A residual jitter of 0.14 arcsec has been achieved. The error rejection bandwidth of the system can be adjusted in the range from 5 Hz to 28 Hz according to the beacon size and the strength of the atmospheric turbulence.

Acknowledgements This work was funded by the National Natural Science Foundation of China under the contact No. 19789301.

References

Ballesteros E., Collados M., Bonet J. A., Lorenzo F., Viera T., Reyes M., Rodriguez Hidalgo I., 1996, A&AS, 115, 353

Molodij G., Rayrole J., Madec P. Y., Colson F., 1996, A&AS, 118, 169

Rao C. H., Jiang W. H., Ling N., Beckers J. M., 2001, Acta Astronomica Sinica, 42, 329

Rao C. H., Jiang W. H., Ling N., Beckers J. M., 2002, Proc. SPIE, 4494, 245

Rao C. H., Jiang W. H., Fang C. et al., 2003, Proc. of SPIE, 4853, 658

Rimmele T. R., Radick R. R., 1998, Proc. SPIE, 3353, 72

von der Luehe O., Widener A. L., Rimmele T. R. et al., 1989 , A&A, 224, 351